



Inhibition of HIV-1 capsid assembly: Optimization of the antiviral potency by site selective modifications at N1, C2 and C16 of a 5-(5-furan-2-yl-pyrazol-1-yl)-1H-benzimidazole scaffold

Martin Tremblay^{a,*}, Pierre Bonneau^a, Yves Bousquet^a, Patrick DeRoy^a, Jianmin Duan^a, Martin Duplessis^a, Alexandre Gagnon^{b,†}, Michel Garneau^a, Nathalie Goudreau^a, Ingrid Guse^a, Oliver Hucke^a, Stephen H. Kawai^{a,§}, Christopher T. Lemke^a, Stephen W. Mason^{c,‡}, Bruno Simoneau^a, Simon Surprenant^a, Steve Titolo^a, Christiane Yoakim^a

^aBoehringer Ingelheim (Canada) Ltd, Research & Development, Laval, Québec, Canada H7S 2G5

^bUniversité du Québec à Montréal, Département de Chimie, C.P. 8888, Succ. Centre-Ville, Montréal, Québec, Canada H3C 3P8

^cBristol-Myers Squibb, Virology, 5 Research Parkway, Wallingford, CT 06492, USA

ARTICLE INFO

Article history:

Received 27 August 2012

Revised 2 October 2012

Accepted 8 October 2012

Available online 16 October 2012

Keywords:

HIV-1

Capsid assembly inhibitor

Benzimidazole

X-ray crystal structure

ABSTRACT

A uHTS campaign led to the discovery of a 5-(5-furan-2-ylpyrazol-1-yl)-1H-benzimidazole series that inhibits assembly of HIV-1 capsid. Synthetic manipulations at N1, C2 and C16 positions improved the antiviral potency by a factor of 1000. The X-ray structure of 33 complexed with the capsid N-terminal domain allowed identification of major interactions between the inhibitor and the protein.

© 2012 Elsevier Ltd. All rights reserved.

The United Nations World Health Organization estimated that in 2009 the population infected by HIV had reached 33 million individuals with 2 million AIDS-related deaths per year.¹ Since the discovery of the virus in 1981, more than 26 FDA-approved drugs have been added to the antiretroviral arsenal against HIV. The current standard of care is a multi-drug therapeutic regime, often referred to as highly active antiretroviral therapy (HAART). The development of HAART has considerably improved the life expectancy of HIV positive patients over the past 25 years.² Although, the HAART regime can efficiently inhibit viral replication for many years, drug resistance still occurs, resulting in a continuing need for the development of novel HIV inhibitors. In addition to inhibiting new targets within the HIV replication cycle, these compounds must also deliver safe toxicological profiles and be compatible with long-term treatment.³

* Corresponding author. Tel.: +1 450 682 4640; fax: +1 450 682 4189.

E-mail address: martin.tremblay@boehringer-ingelheim.com (M. Tremblay).

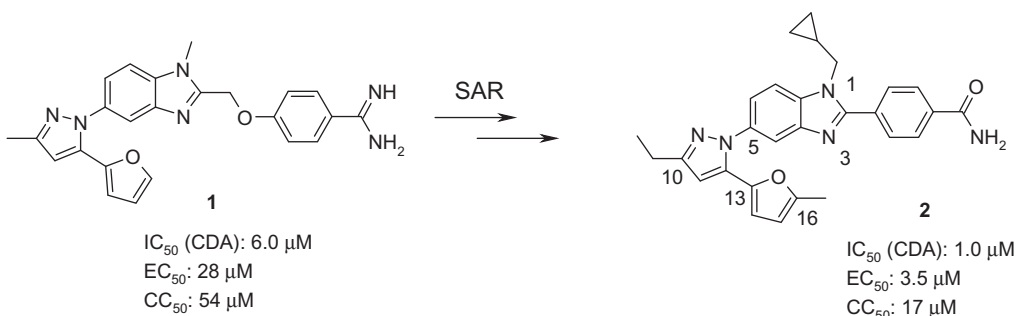
[†] Present address.

[‡] Present address.

[§] Current address: Department of Chemistry and Biochemistry, Concordia University, 7141 Sherbrooke Street W., Montreal, Quebec, Canada H4B 1R6. Tel.: +1 514 848 2424x3331.

The HIV-1 capsid protein (CA), which plays an essential role in both the early and late phases of the HIV life cycle, is a promising novel antiviral target.⁴ During viral maturation, proteolytic cleavage of the 55-kDa Gag polyprotein releases CA, which reassembles to form a cone shaped structure that encloses the viral RNA genome and all the enzymatic activities required for future rounds of infection. The proper assembly of CA is essential for HIV infectivity since CA mutations that prevent core assembly result in non-infectious viral particles.⁵ CA is comprised of two independently folding domains, an N-terminal domain (CA_{NTD}) and a C-terminal domain (CA_{CTD}), which are separated by a short flexible linker. CA_{NTD} self-associates into hexameric rings which are further reinforced by intermolecular CA_{NTD}–CA_{CTD} interactions. In addition, intermolecular CA_{NTD}–CA_{CTD} interactions made between adjacent CA proteins of a hexamer reinforce the basic hexamer unit. Finally homodimeric CA_{CTD}–CA_{CTD} interactions allow each hexamer to interact with six neighboring hexamers, thereby perpetuating the hexagonal lattice.⁶ Pioneering work by Sundquist and coworkers⁷ led to the discovery that CA can assemble into cone-like particle in vitro, which allowed for the identification by us^{8a,b} and others^{8c–k} of small molecule CA inhibitors.

Screening of our corporate compound collection with our capsid assembly assay (CAA)^{8a} led to the identification of benzimidazole 1



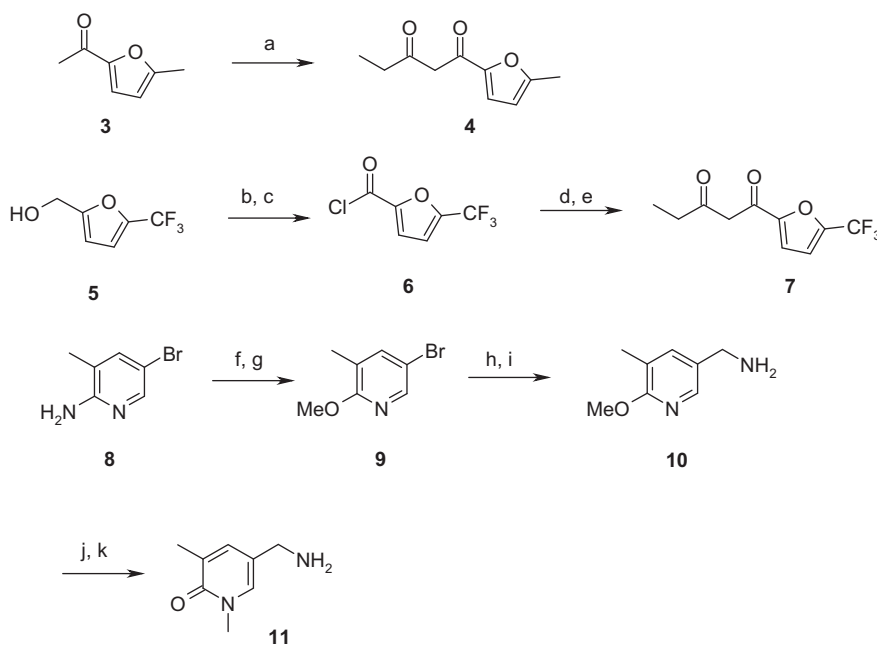
Scheme 1.

(Scheme 1).⁹ With an assay wall¹⁰ of approximately 200–400 nM, the resolution of CAA was not enough for this series optimization. Consequently, the capsid disassembly assay (CDA)¹¹ has been developed to follow our structure-activity relationship. This new assay improved by a factor of 10 the assay wall and was used during the program. Benzimidazole **1** showed a modest IC_{50} (CDA) value of 6 μ M, but no detectable antiviral activity (CC_{50}/EC_{50} ~twofold).¹² We began hit-to-lead efforts to address the optimizability of the scaffold, improve potency in the CDA and identify compounds with clear antiviral potency. We rapidly realized that substitution on the furfurylpyrazole moiety was limited to an ethyl at C10. On the other hand, N1 and C2 positions of the benzimidazole scaffold were found to be very permissive, which we hoped would help improve the potency of the series. Replacing substituent at C2 with a 4-benzamide group and having a cyclopropylmethyl group at N1 led to the identification of compound **2**, which exhibited an IC_{50} value of 1.0 μ M and possesses clear antiviral activity with an EC_{50} value of 3.5 μ M (CC_{50} = 17 μ M).¹³ This communication describes the antiviral potency optimization by site selective modification at positions N1, C2 and C16.

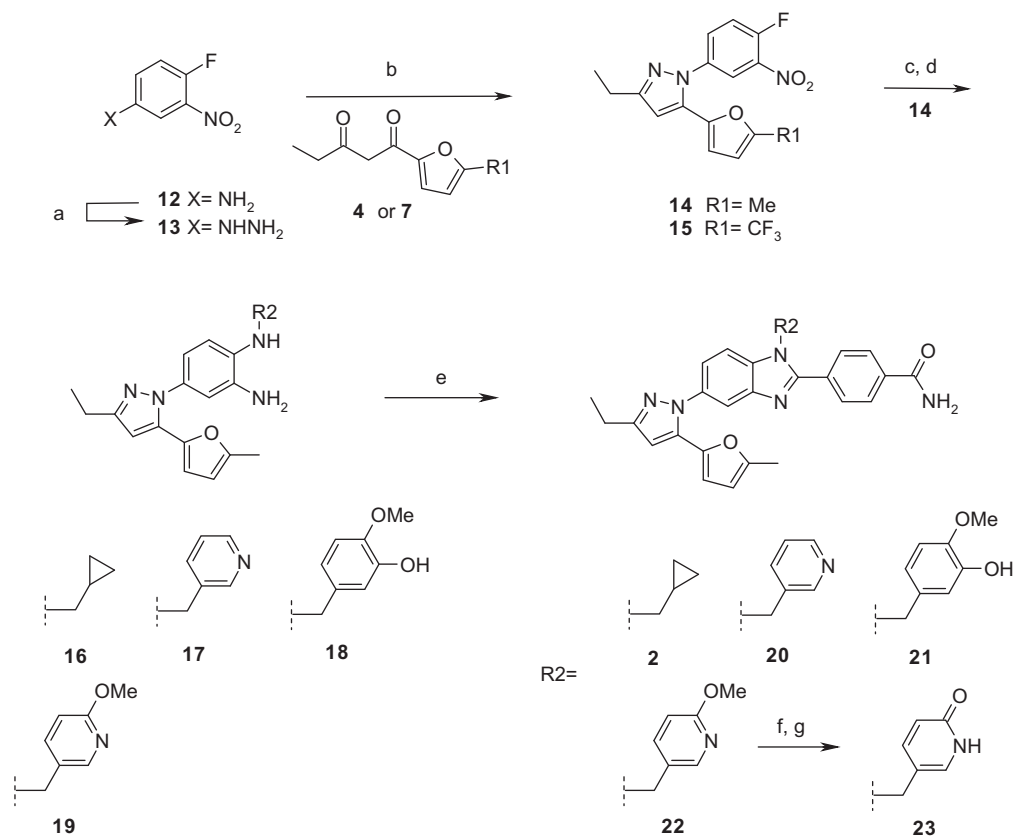
Synthesis of the building blocks started with the alkylation of the anion of 2-acetyl-5-methylfuran **3** with propanoyl chloride to

give the corresponding diketone **4** (Scheme 2). Diketone **7** was synthesized using trifluoromethylfuran derivative **5**. Oxidation of the alcohol **5** to the corresponding acid, followed by treatment with oxalyl chloride, led to acyl chloride **6**. Alkylation of the anion of *tert*-butyl propionoacetate with **6** followed by acidic decarboxylation gave the desired diketone **7**. The 2-aminopyridine **8** was converted to the 2-methoxypyridine **9** via the formation of the corresponding pyridone followed by regioselective O-methylation. Coupling of 5-bromopyridine **9** in the presence of CuCN followed by hydrogenation led to desired pyridinemethylamine **10**. Temporary protection of the primary amine of **10** as a *tert*-butyloxycarbonyl derivative, followed by simultaneous methylation/deprotection gave pyridinemethylamine **11**.

The preparation of inhibitors started with diazotization of **12** followed by tin reduction to give the corresponding hydrazine **13** (Scheme 3). Acidic condensation with diketone **4** and **7** led to pyrazoles **14** and **15**, respectively, with complete regioselectivity. Simple aromatic nucleophilic substitution with different amines followed by reduction of the nitro group using Sn/HCl gave diamines **16–19**. The benzimidazole ring system was easily obtained using a condensation/oxidation methodology developed in our laboratories.¹⁴ Consequently, the obtained diamines **16–19** were



Scheme 2. (a) LDA, propanoyl chloride, THF, -78 °C then RT, 90%; (b) Dess–Martin periodinane, CH_2Cl_2 , then $NaClO_2$, 2-methyl-2-butene, *t*-BuOH, phosphate buffer pH 7, quant.; (c) oxalyl chloride, CH_2Cl_2 , cat. DMF, 0 °C, 99%; (d) *tert*-butyl propionoacetate, Et_3N , $MgCl_2$, MeCN; (e) TFA, CH_2Cl_2 , 60% (2 steps); (f) $NaNO_2$, H_2SO_4 , H_2O , 0 °C to RT, 67%; (g) MeI, Ag_2CO_3 , CH_2Cl_2 , quant.; (h) CuCN, DMF, 130 °C, 81%; (i) H_2 , Pd/C 10%, aq. HCl, MeOH, quant.; (j) $(Boc)_2O$, Et_3N , CH_2Cl_2 , 87%; (k) MeI, CH_2Cl_2 , sealed tube 120 °C, 48 h, quant.



Scheme 3. (a) NaNO₂, HCl, SnCl₂, –25 °C to RT, 55%; (b) diketone **4** or **7**, AcOH, 70–80%; (c) R₂–NH₂, Et₃N, THF, 70–98%; (d) Sn, aq. HCl, THF, quant.; (e) 4-formyl-benzamide, oxone, DMF, H₂O, 6–61%; (f) 33% HBr/AcOH, 100 °C; (g) NH₃/dioxane, TBTU, Et₃N, DMF, 6%.

cyclized using 4-formylbenzamide with Oxone[®] as the oxidant to give **2** and **20–22**, respectively. Deprotection of the methoxypyridine **22** was accomplished by using 33% HBr in AcOH, which also cleaved the amide to the acid. Consequently, simple amide coupling using ammonia in dioxane and TBTU led to **23**.

A series of 2-hydroxybenzaldehydes were condensed with diamine **18** to yield benzimidazoles **24–26** (Scheme 4). Acid **26** was coupled with dimethylamine using TBTU to give amide **27**. Similarly diamine **19** was converted to benzimidazoles **28–30**. Deprotection of the methoxypyridines to the pyridones was achieved upon treatment with HBr in AcOH to give **31–33**, respectively. Finally, acid **33** was also converted into the corresponding dimethylamide **34** as described above.

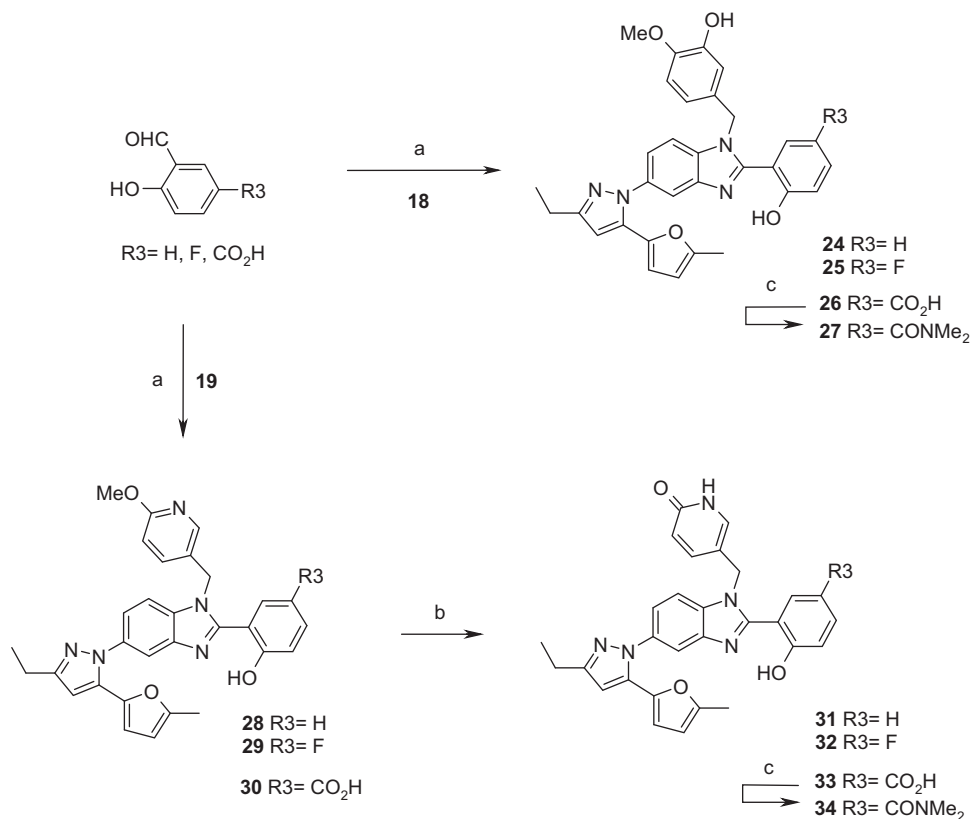
Intermediates **35–37** were obtained from S_NAr substitution by different amines on trifluoromethylfuran analogue **15** followed by reduction and condensation with 3-formyl-4-hydroxybenzoic acid as described above. The methoxypyridines **35** and **36** were converted to the corresponding pyridones using HBr in AcOH and amide coupling led to inhibitors **38–41**. (Scheme 5)

We rapidly found that introduction of substituted aryls and 3-pyridines were well tolerated at the N1 position (Table 1). Replacement of the cyclopropylmethyl group in **2** by a 3-pyridinemethyl substituent (inhibitor **20**) resulted in a threefold gain in potency in the CDA. The 2-methoxyphenol and methoxypyridine derivatives **21** and **22** exhibited similar IC₅₀ values but **21** was found to be significantly more potent in the antiviral assay with an EC₅₀ value of 0.64 μM. The pyridone derivative **23** gave the most potent inhibitor in the CDA with an IC₅₀ value of 0.17 μM. Surprisingly, this modification led to a significant loss in antiviral potency (EC₅₀ = 13 μM). Although poor potency in our cell-based assay was measured, substituted pyridone side chain was later

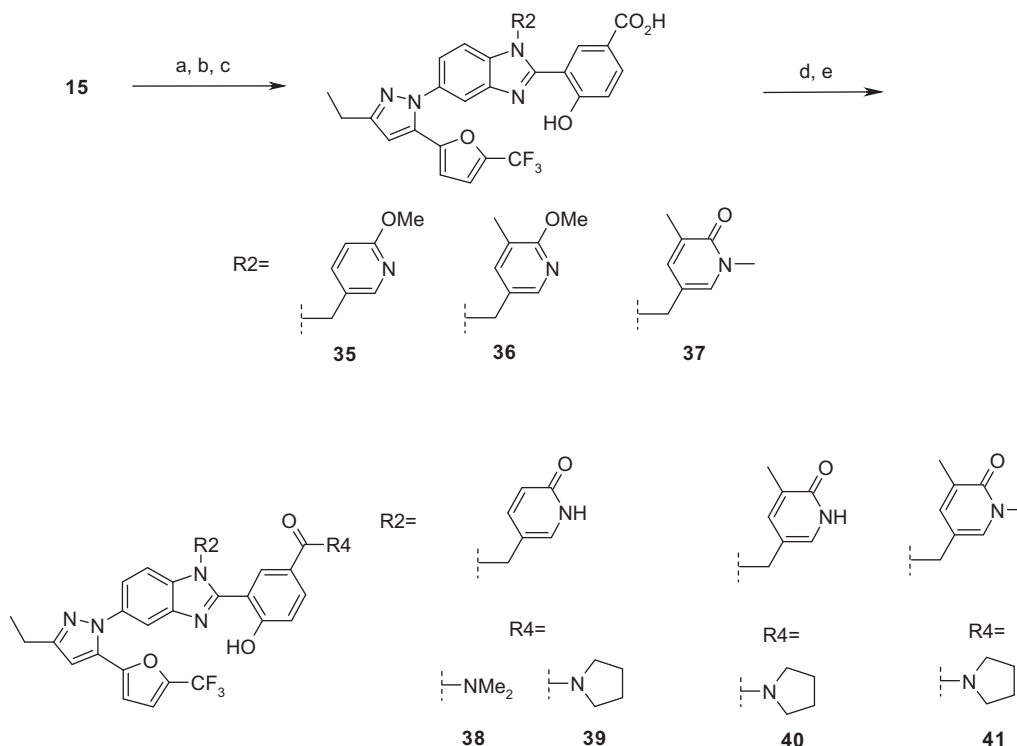
found crucial to improve the antiviral activity when different aryls are introduced at C2.

Keeping the N1 2-methoxyphenol side chain that produced the most potent inhibitor (**21**) in the antiviral assay, we investigated the C2 position (Table 1). Replacement of the 4-benzamide moiety in **21** with a 2-hydroxyphenyl substituent led to **24**, which was found to be twofold more potent in the CDA. Reintroducing electron-withdrawing groups on the 2-hydroxyphenol moiety was found to be beneficial for potency. Incorporating a fluorine atom at the 5 position (**25**) gave a slight gain in intrinsic potency in comparison with **24**. Adding an acid (**26**) or an amide group (**27**) at this position resulted in substantial gain in potency in the CDA. On the other hand, antiviral potency could not be improved further with these 2-methoxyphenol N1 side chains. In contrast with the pyridone analog **23**, introduction of these 2-hydroxyphenyl groups at C2 had a positive impact on both intrinsic and antiviral potencies. Inhibitors **31**, **32** and **34** exhibited a 20- to 50-fold gain in the antiviral assay compared with **23**. These analogues were at the limit of the resolution of the CDA, necessitating development of a more sensitive assay. A fluorescence polarization (FP)¹⁵ displacement assay was therefore developed, with a fluorescein competition onto the carboxylate of **33**. With a K_d of 0.088 μM, this competition assay improved the assay wall to approximately 0.014 μM.

The X-ray structure of **33** complexed with CA_{NTD} confirmed CA as the target of the series and revealed the intermolecular interactions leading to compound binding.¹⁶ The inhibitor induces the formation of a pocket at the base of CA_{NTD} (Fig. 1). The structural movements and functional effects accompanying the formation of this pocket are described elsewhere.^{8a} The furylpyrazole moiety is buried most deeply in the pocket, thus explaining the observed



Scheme 4. (a) Oxone, DMF, H₂O, 8–72%; (b) 33% HBr/AcOH, 100 °C, 17–45%; (c) Me₂NH, TBTU, Et₃N, THF, 14–25%.



Scheme 5. (a) R₂-NH₂, Et₃N, THF, 70–98%; (b) Sn, aq. HCl, THF, quant.; (c) 3-formyl-4-hydroxybenzoic acid, Oxone, DMF, H₂O, 90–98%; (d) 33% HBr/AcOH, 100 °C, quant. (only for **35** and **36**); (e) dimethylamine or pyrrolidine TBTU, Et₃N, THF, 26–60%.

sensitivity of this region to modification. Interactions within the pocket are largely hydrophobic, with the exception of a key

hydrogen bond between the pyrazole and the backbone NH of displaced residue Phe-32. The benzimidazole moiety stacks between

Table 1
Activities and cytotoxicity of substituted benzimidazole derivatives

Compound	IC ₅₀ CDA (μM)	IC ₅₀ FP (μM)	EC ₅₀ (μM)	CC ₅₀ (μM)
1	6.0	—	28	54
2	1.0	—	3.5	17
20	0.36	—	2.6	19
21	0.79	—	0.64	12
22	0.83	—	3.5	13
23	0.17	—	13	>39
24	0.41	—	6.4	>22
25	0.28	—	10	>21
26	0.088	0.55	6.1	>46
27	0.12	—	0.63	16
31	0.055	0.69	0.26	>26
32	0.041	—	0.26	>16
33	0.056	0.65	>46	>46
34	0.049	0.044	0.59	>23
38	—	0.059	0.091	>23
39	—	0.061	0.062	20
40	—	0.038	0.028	18
41	—	0.067	0.027	21

the aromatic sidechains of Phe-32 and His-62, orienting N1 and C2 substituents toward solvent, and positioning N3 for a water-mediated hydrogen bond with the backbone NH of Ala-65. The N1 pyridone lies along the surface of the protein, contacting the side-chains of Ala-31 and Phe-32. The N2 benzoic acid moiety protrudes directly into solvent, with the phenolic oxygen reaching back to form a hydrogen bond with His-62. It is important to note that portions of the inhibitor that are observed as solvent exposed when bound to CA_{NTD} may well form important protein interactions in the context of full length, assembled CA.

Using inhibitor **34** as starting point, the C16 position was revisited and it was found that replacing the methyl substituent by a trifluoromethyl group (cf. **34** and **38** in Table 1) gave a sixfold gain in antiviral potency although there was little impact on the IC₅₀ values. Further modification of the amide group led to the identification of pyrrolidine amide derivative **39** which exhibited IC₅₀ and EC₅₀ values of 61 and 62 nM, respectively. This analogue showed poor metabolic stability upon incubation with rat and human liver

microsomes (45 and 30 min, respectively) and a poor Caco-2 permeability of 0.19×10^{-6} cm/s. N-methylation of the pyridone resulted in an additional twofold gain in antiviral potency for inhibitor **40**. Similar potency was observed with the introduction of another methyl group on the pyridone at position 6 (analogue **41**). These modifications also had a beneficial impact on the Caco-2 permeability, with increases to 6.8 and 7.2×10^{-6} cm/s for compound **40** and **41**, respectively. Unfortunately, microsome stability was reduced by these substitutions. In these cases, metabolic stability upon incubation with rat and human liver microsomes were 25 and 11 min. for **40** and 18 and 10 min. for **41**, respectively.

In conclusion, we have demonstrated that the inhibition of HIV capsid assembly is a valid approach to inhibit HIV replication. We have optimized a hit compound with no measurable antiviral activity to an advanced lead compound with an EC₅₀ value of 27 nM, which is the most potent HIV capsid assembly inhibitor reported to date. The synthetic approach allowed diversification at N1 and C2 positions. We discovered that introduction of a pyridone side chain at N1, a 2-hydroxyphenyl appendage at C2 and a C16 trifluoromethyl group were crucial for improving the antiviral potency. The crystal structure of **33** complexed with CA_{NTD} identified interactions between the inhibitor and the protein that were consistent with the observed SAR. Though promising, this series was unfortunately stopped because of poor metabolic stability, pharmacokinetic profile and limited SAR opportunities to address these liabilities.

Acknowledgments

The authors would like to acknowledge Jean-François Mercier and Elizabeth Wardrop for IC₅₀ and EC₅₀ value determinations, respectively, and Normand Aubry, Colette Boucher, Michael Little and Serge Valois for analytical support. We are also grateful to Michael Bös, Richard Bethell and Michael Cordingley for leadership and guidance in chemistry and biology. Finally, we extend our gratitude to Professor Wesley Sundquist for helpful discussions at the early stage of this project.

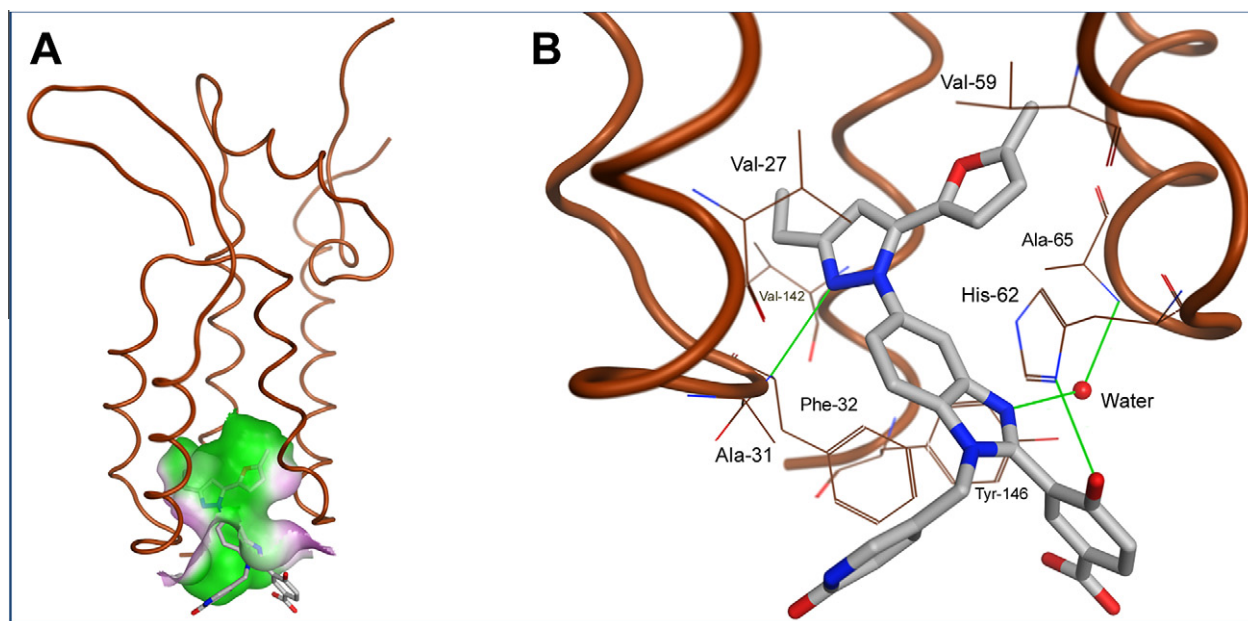


Figure 1. Binding of **33** to CA_{NTD}. (A) Location and surface representation of the binding pocket on CA_{NTD}. CA_{NTD} is illustrated in ribbon-form and **33** is shown as sticks. Lipophilic, neutral and hydrophilic surfaces are colored green, white and pink, respectively. (B) Details of **33** binding. Representations are similar to A, with the addition of interacting residues in lineform, hydrogen bonds as green lines, an ordered water molecule as a red sphere and some residues in the foreground were removed for clarity.

References and notes

- UNAIDS/WHO "AIDS Epidemic Update 2009", November 2009, Geneva. http://data.unaids.org/pub/Report/2009/JC1700_Epi_Update_2009_en.pdf (accessed May 2012).
- For a recent review about the impact of antiretroviral therapy on HIV pandemic, see: Broder, S. *Antiviral Res.* **2010**, *85*, 1.
- (a) Adamson, C. S.; Freed, E. O. *Antiviral Res.* **2010**, *85*, 119; (b) Flexner, C. *Nat. Rev. Drug Disc.* **2007**, *6*, 959.
- (a) Neira, J. L. *FEBS J.* **2009**, *276*, 6110; (b) Zhang, J.; Liu, X.; De Clercq, E. *Mini-Rev. Med. Chem.* **2009**, *9*, 510; (c) Adamson, C. S.; Salzwedel, K.; Freed, E. O. *Expert Opin. Ther. Targets* **2009**, *13*, 895; (d) Ganser-Pornillos, B. K.; Yeager, M.; Sundquist, W. I. *Curr. Opin. Struct. Biol.* **2008**, *18*, 203.
- (a) Ganser-Pornillos, B. K.; von Schwedler, U. K.; Stray, K. M.; Aiken, C.; Sundquist, W. I. *J. Virol.* **2004**, *78*, 2545; (b) von Schwedler, U. K.; Stray, K. M.; Garrus, J. E.; Sundquist, W. I. *J. Virol.* **2003**, *77*, 5439; (c) Forshey, B. M.; von Schwedler, U.; Sundquist, W. I.; Aiken, C. *J. Virol.* **2002**, *76*, 5667.
- (a) Pornillos, O.; Ganser-Pornillos, B. K.; Yeager, M. *Nature* **2011**, *469*, 424; (b) Pornillos, O.; Ganser-Pornillos, B. K.; Kelly, B. N.; Hua, Y.; Whitby, F. G.; Stout, C. D.; Sundquist, W. I.; Hill, C. P.; Yeager, M. *Cell* **2009**, *137*, 1282; (c) Ganser-Pornillos, B. K.; Yeager, M.; Sundquist, W. I. *Curr. Opin. Struct. Biol.* **2008**, *18*, 203.
- Sundquist, W. I.; Wang, H.; Hill, C. P.; Stemmler, T. L.; Davis, D. R.; Alam, S. *PCT Int. Appl. WO 2003013425*, 2003.
- (a) Lemke, C. T.; Titolo, S.; von Schwedler, U.; Goudreau, N.; Mercier, J.-F.; Wardrop, E.; Faucher, A.-M.; Coulombe, R.; Banik, S.; Fader, L. D.; Gagnon, A.; Kawai, S.; Rancourt, J.; Tremblay, M.; Yoakim, C.; Simoneau, B.; Archambault, J.; Sundquist, W. I.; Mason, S. W. *J. Virol.* **2012**, *86*, 6643; (b) Fader, L. D.; Bethell, R.; Bonneau, P.; Bös, M.; Bousquet, Y.; Cordingley, M. G.; Coulombe, R.; DeRoy, P.; Faucher, A.-M.; Gagnon, A.; Kawai, S. H.; Lacoste, J.-E.; Landry, S.; Lemke, C. T.; Malenfant, E.; Morin, S.; O'Meara, J.; Simoneau, B.; Yoakim, C. *Bioorg. Med. Chem.* **2011**, *21*, 398; (c) Tian, B.; He, M.; Tan, Z.; Tang, S.; Hewlett, I.; Chen, S.; Jin, Y.; Yang, M. *Chem. Biol. Drug Des.* **2011**, *77*, 189; (d) Shi, J.; Zhou, J.; Shah, V. B.; Aiken, C.; Whitby, K. *J. Virol.* **2011**, *85*, 542; (e) Blair, W. S.; Pickford, C.; Irving, S. L.; Brown, D. G.; Anderson, M.; Bazin, R.; Cao, J.; Ciaramella, G.; Isaacson, J.; Jackson, L.; Hunt, R.; Kjerrstrom, A.; Nieman, J. A.; Patick, A. K.; Perros, M.; Scott, A. D.; Whitby, K.; Wu, H.; Butler, S. L. *PLoS Pathog.* **2010**, *6*, e1001220; (f) Li, J.; Tan, Z.; Tang, S.; Hewlett, I.; Pang, R.; He, M.; He, S.; Tian, B.; Chen, K.; Yang, M. *Bioorg. Med. Chem.* **2009**, *17*, 3177; (g) Kelly, B. N.; Kyere, S.; Kinde, I.; Tang, C.; Howard, B. R.; Robinson, H.; Sundquist, W. I.; Summers, M. F.; Hill, C. P. *J. Mol. Biol.* **2007**, *373*, 355; (h) Prevelige, P. *WO 2007048042*, 2007; (i) Sticht, J.; Humbert, M.; Findlow, S.; Bodem, J.; Muller, B.; Dietrich, U.; Werner, J.; Krausslich, H. G. *Nat. Struct. Mol. Biol.* **2005**, *12*, 671; (j) Ternois, F.; Sticht, J.; Duquerry, S.; Krausslich, H. G.; Rey, F. A. *Nat. Struct. Mol. Biol.* **2005**, *12*, 678; (k) Tang, C.; Loeliger, E.; Kinde, I.; Kyere, S.; Mayo, K.; Barklis, E.; Sun, Y.; Huang, M.; Summers, M. F. *J. Mol. Biol.* **2003**, *327*, 1013.
- Yoakim, C.; DeRoy, P.; Duplessis, M.; Gagnon, A.; Goulet, S.; Hücke, O.; Lemke, C.; Surprenant, S. *PCT Int. Appl. WO 2008/067644*, 2008.
- The assay well corresponds to the minimal measured IC₅₀ value and usually can be approximated by half target protein concentration.
- Reacti-Bind Neutravidin Coated Black 384-Well plates (Pierce Cat# 15402) were first washed with 80 µl/well of Buffer A (50 mM Tris pH 8.0; 350 mM NaCl; 10 µM ZnSO₄; 0.0025% CHAPS (w/v); 50 µg/ml BSA; 1 mM DTT). Immobilization of a 5'-end biotin labeled (TG)₂₅ oligonucleotide (Integrated DNA Technology Inc.) was then carried out by adding 50 µl/well of a 25 nM solution of oligonucleotide in Buffer A + 5 mg/ml BSA and incubating overnight. Unbound material was removed by two 80 µl/well washes with Buffer A. Assembly reactions were performed in 60 µl/well reactions comprising 100 nM of 5'-end fluorescein labeled (TG)₂₅ oligonucleotide (Integrated DNA Technology Inc.) and 2 µM of CA-NC protein, using Buffer A. Assembly reactions were incubated for 2 h at room temperature and non-immobilized material was removed by washing 80 µl/well with Buffer A. Test compounds, serially diluted in Buffer A + 0.125% DMSO, were added to the wells (60 µl/well) and incubated at room temperature for 2 h. Disassembled material was removed by two successive 80 µl/well washes with Buffer A. Finally, 80 µl/well of Buffer A + 0.1% SDS was added and incubated for 15 minutes prior to quantification of captured fluorescence on a Victor plate reader (Perkin Elmer Life Sciences) equipped with fluorescein excitation and emission filters. The capacity of a test compound to dissociate assembled complexes was considered proportional to the observed loss of captured fluorescence. The IC₅₀ values for each compound were generated by fitting disassembly curves from ten-point dilution series to the following equation: %inhibition($(I_{\max}^n \times [I]^n) \div ([I]^n + IC_{50}^n)$) × 100, and represent the concentration of compound required for 50% disassembly.
- Cytotoxicity concentration (CC₅₀) is defined as the concentration resulting in the death of 50 percent of the host cells and antiviral potency (EC₅₀) as the concentration inhibiting virus replication by 50 percent.
- All the compounds described have a cytotoxicity window (or selectivity index) greater than 5.
- Beaulieu, P. L.; Haché, B.; von Moos, E. *Synthesis* **2003**, 1683.
- Serial dilutions of test compounds in FP buffer (50 mM Tris pH 8.0; 100 mM NaCl; 0.0025% CHAPS; 1 mM DTT) + 2% DMSO were added (40 µl) to a Corning 384-well black non-binding polystyrene plate. Reactions were completed by adding 40 µl of a solution containing CA-NC protein (40 nM) and fluorescein-labeled probe linked onto the carboxylate of **33** (40 nM) in FP buffer. Plates were incubated for 15 minutes prior to reading on a Victor plate reader (Perkin Elmer Life Sciences) using a fluorescence polarization protocol for fluorescein. Control wells (absence of test compound) and blank wells (only probe) were included on each plate, representing 0% and 100% displacement, respectively. The IC₅₀ values for each compound were generated by fitting displacement curves from ten-point dilution series to the following equation: %inhibition($(I_{\max}^n \times [I]^n) \div ([I]^n + IC_{50}^n)$) × 100, and represent the concentration of compound required for 50% displacement of the probe.
- Protein Data Bank (PDB) ID: 4E92.